Multivariate analysis of EEG activity indexes contingent attentional capture

Jaap Munneke [a,b,c,1,*], Johannes Jacobus Fahrenfort [c,1], David Sutterer [d], Jan Theeuwes [c], Edward Awh [e,f]

[a] College of Health, Medicine and Life Sciences, Brunel University London, Kingston Lane, UB8 3PH Uxbridge, UK
[b] Centre for Cognitive Neuroscience, Brunel University London, UK
[c] Department of Experimental and Applied Psychology, Institute for Brain and Behavior, Vrije Universiteit Amsterdam, the Netherlands
[d] Department of Psychology, Vanderbilt University, USA
[e] Department of Psychology, University of Chicago, USA
[f] Institute for Mind and Biology, University of Chicago, USA

ARTICLE INFO

ABSTRACT

An extensive body of work has shown that attentional capture is contingent on the goals of the observer: Capture is strongly reduced or even eliminated when an irrelevant singleton stimulus does not match the target-defining properties (Folk et al., 1992). There has been a long-standing debate on whether attentional capture can be explained by goal-driven and/or stimulus-driven accounts. Here, we shed further light on this matter by using EEG activity (raw EEG and alpha power) to provide a time-resolved index of attentional orienting towards salient stimuli that either matched or did not match target-defining properties. A search display containing the target stimulus was preceded by a spatially uninformative singleton cue that either matched the color of the upcoming target (contingent cues), or that appeared in an irrelevant color (non-contingent cues). Multivariate analysis of raw EEG and alpha power revealed preferential tuning to the location of both contingent and non-contingent cues, with a stronger bias towards contingent than non-contingent cues. The time course of these effects, however, depended on the neural signal. Raw EEG data revealed attentional orienting towards the contingent cue early on in the trial (>156 ms), while alpha power revealed sustained spatial selection in the cued locations at a later moment in the trial (>250 ms). Moreover, while raw EEG showed stronger capture by contingent cues during this early time window, an advantage for contingent cues arose during a later time window in alpha band activity. Thus, our findings suggest that raw EEG activity and alpha-band power tap into distinct neural processes that index separate aspects of covert spatial attention.

Introduction

Two opposing views of attentional capture can be distinguished, based on the degree to which the internal goals of an observer influence this process. Some have argued for a fully stimulus-driven, bottom-up account of attentional capture in which attention is automatically and involuntarily allocated to the location of a salient stimulus such as an abrupt onset (Schreij et al., 2008, 2010) or a stimulus with unique visual features such as its color or luminance (Kim and Cave, 1999; Theeuwes, 1991, 1992, 2004), which makes the stimulus "pop-out" from its surrounding elements. By contrast, others have argued that attentional capture is contingent on an observer's current target template. This phenomenon is known as feature-based contingent capture and refers to the observation that attention is automatically captured by task-irrelevant stimuli that share vital visual features with the target

stimulus (Bacon and Egeth, 1994; Egeth and Yantis, 1997; Folk et al., 1992; Folk and Remington, 1998; Leber and Egeth, 2006; Wolfe et al., 2003).

Contingent capture was originally observed in a study by Folk et al. (1992) in which participants were instructed to detect a target that was either defined based on its color (e.g. a red character among white characters) or by its presentation as an abrupt onset. Shortly (150 ms) before presenting the target display, a brief cue display was presented consisting of a color or an abrupt onset stimulus, presented at one of four possible target locations. The cue location was task-irrelevant and did not predict the subsequent target location. The critical observation was that only a cue that shared critical features with the expected target stimulus captured attention, resulting in a strong spatial validity effect (i.e. faster response times when the cue correctly indicated the target location, as compared to when cue and target were presented at

* Corresponding author at: College of Health, Medicine and Life Sciences, Brunel University London, Kingston Lane, UB8 3PH Uxbridge, UK.
E-mail address: Jaap.Munneke@brunel.ac.uk (J. Munneke).
[1] These authors contributed equally.

different spatial locations). Crucially, when participants were searching for a target defined by an abrupt onset, a red cue amongst white distractors did not show evidence of attentional capture, whereas this cue did capture attention when participants were searching for a red target. This finding was taken as evidence that attentional capture is not solely driven by bottom-up processes, but that feature-based attentional mechanisms are instrumental as well (but see Belopolsky et al., 2010).

Recent EEG work has provided converging evidence that attentional capture is contingent on the observer's feature-based top-down set by measuring the N2pc component. This event-related potential (ERP) component indexes the visual hemifield in which a selected item appears. The N2pc is a negative deflection that onsets approximately 200 ms after stimulus onset and is observed over the parieto-occipital scalp sites contralateral to selected visual stimuli. Eimer and Kiss (2008) showed that the N2pc was elicited in response to a salient and contingent (i.e. target matching) cue, but only when the target was presented among distractors. Further evidence that the N2pc reflects feature-based attentional processes was provided in a recent study by Grubert et al. (2017). They showed that non-salient stimuli elicited an N2pc component, but only when these stimuli shared critical features with the target *and* the observer was actively searching for this target. However, when the target was already found and the target template was no longer active, the same non-salient stimuli did not evoke an N2pc. The findings observed by Grubert and colleagues were taken as evidence that the N2pc indeed reflects feature-based attentional processes, and the absence of an N2pc when the observer is not actively searching for a target cannot be explained in terms of bottom-up attention (but see Hickey et al., 2006, for a bottom-up interpretation of the N2pc).

Thus, EEG evidence has suggested that an observer's target template influences attentional allocation by showing a direct relationship between the N2pc and feature-based attentional capture. However, one of the shortcomings of using the N2pc as an index of contingent capture is that it is a transient neural response that occurs approximately 200 ms post stimulus onset, so it does not allow sustained tracking of covert attention during subsequent points in time. In addition, the N2pc as a measure of attentional allocation lacks spatial specificity (Fahrenfort et al., 2017). The N2pc is measured as a difference in electrical potential between two electrodes placed over ipsi- and contralateral cortical regions (relative to a visual stimulus) and as such does not provide information concerning the attended location beyond hemispheric differentiation. These shortcomings, as well as those imposed by purely behavioural research, may impede a proper investigation into the neural mechanisms underlying feature-based contingent capture. Here, we investigate the contingent nature of automatic capture, while simultaneously controlling for bottom-up factors, using a temporally resolved method that tracks attentional allocation throughout the entire cue-target interval. As the data will show, this provides novel insights in the time course of contingent capture, suggesting distinct early and late neural components to contingent capture that appear to serve different functional roles in cue related attentional processes.

To obtain a high-resolution spatiotemporal profile of contingent capture, we tracked the locus of covert attention using the scalp distribution of both raw EEG (Fahrenfort et al., 2017) and alpha power (Foster, Bsales, et al., 2017; Foster et al., 2016; Foster, Sutterer, et al., 2017). Recent work has shown that both signals provide time-resolved and precise tracking of attended locations, making this an ideal approach for understanding temporal dynamics of automatic contingent capture. The current study uses this methodology to characterize the spatiotemporal properties of contingent capture, controlled for bottom-up influences, by investigating how contingent and non-contingent stimuli influence attentional allocation over time. Following previous studies on contingent capture, we utilized a task in which participants were instructed to respond to a target of a pre-defined color. Prior to presenting the search array containing the target, a cue display was used that contained a singleton color cue surrounded by non-singleton grey stimuli. The color of the cue either matched or did not match the color of the target. The

logic here is that both cue types may capture attention due to their singleton status, but only the cue that matched the target color evokes attentional processing related to contingent capture (i.e. capture as a result of having an active target template). By subtracting the neural processes related to non-contingent capture from similar processes related to contingent capture, one is left with a neural index that is solely related to contingent capture, with influences of bottom-up capture removed from this signal. The current study investigates the neural time course of contingent and non-contingent capture, as well as the differences between these two signals (in the absence of bottom-up factors).

We note that phase-locked changes in the raw EEG distributed signal were investigated, whereas non-phase-locked changes were studied in the induced alpha-band power distribution (see Methods). To our knowledge, both neurophysiological correlates of attention (i.e., raw EEG and time-frequency information in the alpha-band range) have not been combined in a single study. Although both neural signals track covert attention and distinguish between contingent and non-contingent cues, our results show the divergent time course of these effects, indicating that these different signals may tap into distinct aspects of contingent capture.

Methods

Participants

We tested 33 participants (22 females; mean age $\pm$ SD = 22.48 $\pm$ 3.21 years) with normal or corrected-to-normal vision. All participants gave written informed consent prior to the start of the experiment. All participants were recruited from the student community of the University of Oregon, USA (25), and the student population of Bilkent University, Turkey (8). Participants received a monetary reward or course credits for completing the experiment. The experimental procedures of this and all subsequent experiments were approved by the ethical committees of the University of Oregon and Bilkent University, and are in accordance with the Declaration of Helsinki.

Out of the 33 tested participants, four had to be discarded for either showing poor behavioral performance (accuracy around chance: one participant) or technical issues during measurement (three participants). All reported analyses below are based on data from the remaining 29 subjects.

Stimuli and procedure

The experiment was conducted at the University of Oregon, USA and Bilkent University, Turkey, with near-identical procedures between the testing locations[1]. Participants were seated in a dimly lit room, at a viewing distance of 65 cm from a 22" CRT computer monitor. Prior to the start of the experiment, a 20-channel EEG electrode cap was fitted on the scalp of the participants and attached to an SA Instrumentation amplifier located in a Faraday cage.

Fig. 1 shows the time course of a typical experimental trial. Participants started the trial by fixating on a centrally presented gray fixation cross (0.3° × 0.3°). After 500 ms, the fixation cross turned black for 100 ms as a general indication that the critical part of the trial had started and that participants should refrain from making eye movements until the end of the trial. The fixation cross turned back to gray for a random period between 800 and 1200 ms (in increments of 100 ms), after which the cue screen was presented. The cue screen consisted of eight circles (2.5° radius) presented in a circular array around fixation with

---

[1] The current method section describes the stimuli and procedure as conducted at the University of Oregon. Equipment used at Bilkent university consisted of a 20" CRT monitor, 20 selected channels on a 64-channel cap connected to a BrainAmp amplifier (Cap and Amplifier: Brain Products GmbH). Crucially, stimulus timing and physical properties (including visual angle), as well as the precise recording electrodes were identical between testing locations.
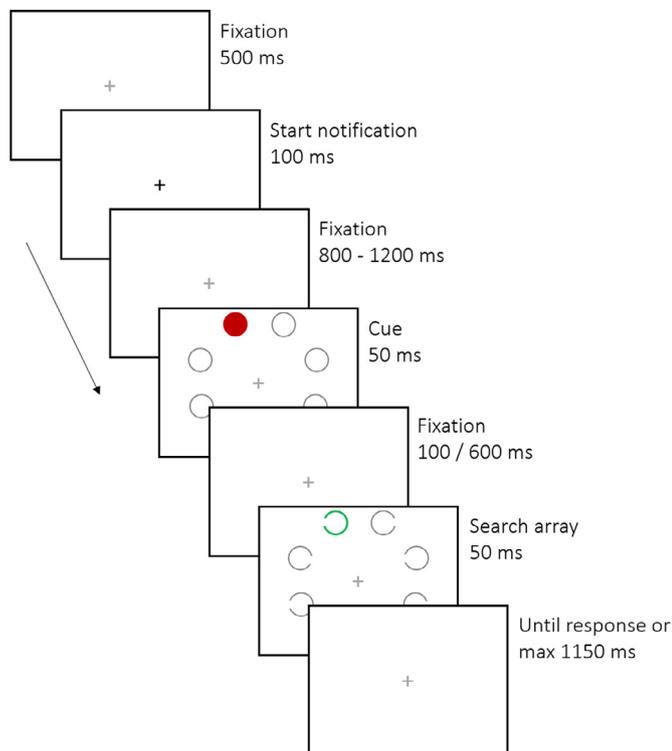
Fig. 1. Time course of a typical experimental trial. In this particular trial, the cue is non-contingent (the colors of the cue and target do not match) and valid (cue and target are presented at the same location).

a radius of 5.0 degrees of visual angle. On each trial, one of the circles was presented as a solid red or green disc (luminance 30 cd/m^2), functioning as a spatially non-predictive cue. As these cues had the same luminance, bottom-up factors that influenced attention were equated between the contingent and non-contingent conditions. After 50 ms, all circles, including the cue, were removed from the screen for either 100 or 600 ms during which only the fixation cross remained present. Following this fixation-only interval the search array was presented for 50 ms, consisting of eight circles, each having a small opening on the right or the left side. On each trial, the target circle was presented in a predefined color that remained constant throughout the experiment (red and green, counterbalanced over participants). Participants were instructed to give a speeded response indicating on which side the circle had a small opening.

Short and long inter-stimulus intervals (Stimulus Onset Asynchrony: SOA) were used such that trials with a short SOAs (cue onset – target onset: 150 ms) reflected classic studies on contingent capture in order to illustrate any behavioral effects. Trials with a long SOA (cue onset – target onset: 650 ms) were used to investigate how contingent and non-contingent cues influenced automatic effects of capture, as well as any spatial biases that were sustained for longer periods of time (up to 1000 ms after cue onset). Trials with short and long SOAs were randomly intermixed in each experimental block.

Cues were either contingent (having the same color as the target) or non-contingent (having a different color as the target). An equal number of contingent and non-contingent cues were used by counterbalancing the number of red and green cues and randomizing their order within the experiment. Furthermore, cue and target location were fully counterbalanced and presented equally often at each of the eight locations in the visual field, resulting in a cue (location) validity of 12.5%. The experiment consisted of 1280 (71.4%) trials with long SOAs and 512 (28.6%) trials with short SOAs. Finally, the eight cue and target locations were not fixed, but could be presented anywhere on the radius around fixation, with the limitation that the inter-stimulus distance re-

mained constant at 4.14° (i.e., the whole display could rotate, but the eight individual circles were always presented equidistant at a 45° angle between the center of the screen and two adjacent stimuli) and that locations were kept constant within a trial. As a result of this 'random' placement, the circle on which the stimuli were presented was divided in eight equally large segments, with each segment representing one location, despite the precise position of a stimulus within this segment. Therefore, we will refer to these segments as locations from here on. The entire session, including EEG preparation took approximately 2.5 hours to complete.

EEG recording and preprocessing

A 20-channel electro-cap (Electro-Cap international) was used to record EEG from the following electrodes: F3, FZ, F4, T3, C3, CZ, C4, T4, P3, PZ, P4, PO3, PO4, PO7, PO8, POZ, T5, T6, O1, and O2. The left mastoid was used as an online reference and all data was re-referenced offline to the average of all electrodes. HEOG was obtained by placing two electrodes at the outer canthi of both eyes, enabling the measurements of horizontal eye movements. VEOG and blinks were measured by placing an electrode above and below the left eye[2]. All incoming signals (EEG and EOG) were amplified and filtered with a bandpass filter of 0.01– 80 Hz. Subsequently, all signals were online resampled at 250 Hz. Impedances were kept below 5 kΩ throughout the experiment. In order to obtain a reliable response to the cue, not modulated by other visual stimulation, only the trials with a long SOA were included in the EEG analyses.

Next, the EEG data was segmented in 2s epochs around cue onset (–500:1500). The contribution of eye blinks to the EEG signal was removed from the epoched data using an independent component analysis (ICA), by removing components that showed clear blink-related activity. Next, all ICA corrected epochs that contained data from trials with behaviorally incorrect responses were removed. The remaining epochs were checked for eye movements made in the time window 0– 650 ms (i.e., from cue onset until target onset). Eye movements were detected by moving a 50 ms window over the preprocessed EEG data in steps of 50 ms within the HEOG or VEOG channels. Amplitude changes of 25 μv within that window were flagged as eye-movements and any trial containing such artifacts were subsequently deleted from the data set (2.95%). Finally, epochs containing muscle artifacts were removed from the data by calculating the z-value of the power values in the EEG signal, for frequencies above 110 Hz (up to 125 Hz). Trials that contained *z*-score outliers more than 3 standard deviations away from the absolute value of the minimum negative *z*-score were marked as containing a muscle artifact and were removed from the data set (3.99%). All preprocessing steps were conducted using EEGLAB (Delorme and Makeig, 2004) and the Amsterdam Decoding and Modeling toolbox (Fahrenfort, van Driel, van Gaal, and Olivers, 2018).

EEG analysis

In order to use alpha power in our analyses, FieldTrip (Oostenveld et al., 2010) was used to decompose the raw EEG signal into frequency-specific power spectra. Frequency-specific power spectra were based on a Fast Fourier Transform (FFT) approach using a fixed (i.e., independent of frequency band) 500 ms moving Hanning window (step size = 8 ms), resulting in a frequency resolution of 2Hz (1/0.5 sec). As such, the FFT analysis resulted in the time-frequency bins for all even frequencies ranging from 2 to 30 Hz (i.e., 2 Hz, 4 Hz, 6 Hz … 30 Hz). We calculated changes in induced (non-phase

---

[2] The procedure for measuring eye movements at Bilkent University was slightly different as it relied on the placement of only one electrode diagonally under the left eye to pick up the HEOG and the VEOG signal. This procedure proved more than capable in picking up horizontal and vertical eye movements as well as eye blinks.

locked) power for each frequency and time point. The study specifically focused on changes in induced power to ensure that stimulus specific phase-locked signals found in the raw EEG were not present in this signal, thus measuring qualitatively different task-related signals than those encoded in the phase-locked EEG. Induced power was computed by subtracting the condition-specific average evoked response (ERP) waveform from each trial of that condition (cue-position and cue-type) prior to computing the signal's power. This method effectively subtracts out the phase-locked part of the signal from every single trial, leaving only stimulus induced power fluctuations of signals that are plausibly already ongoing (hence non-phase locked) when the stimulus appeared. Induced power signals that are computed by subtracting out ERPs prior to time-frequency decomposition have (by algorithmic logic), a different ontology from signals contained in the phase locked, raw EEG. As such, any difference in classification performance between raw EEG and power-based analyses likely reflect expressions from distinct cortical mechanisms. Indeed, evoked (phase-locked) components such as the N2pc are not present in the induced signal, whereas induced signals are often thought to reflect endogenous process that are modulated, but not initiated by external stimulation or task instruction (e.g. David et al., 2006; Hosseini et al., 2015). The subtraction procedure that was used to obtain induced signals was applied separately to training and testing data in each fold, computing condition-specific ERPs for every training and every testing set, as to prevent the ERP subtraction method from inadvertently introducing commonalities into the entire dataset that could drive above-chance decoding across training and testing. Although it would strictly be sufficient to apply this procedure to the training data only, we chose to apply it to the testing set too, eradicating any remnants of phase-locked activity. However, because the test data did not have enough trials to allow the computation of a sufficiently clean ERP, we fitted a spline through test-set ERPs to remove high-frequency noise prior to subtracting them from the single trials in the testing set.

All analyses were multivariate, either applied to the raw EEG or to the time-frequency decomposed induced signal of the EEG. We first used backward decoding models (BDM) to infer whether we could predict the cue location based on the distributed EEG patterns. Next, we applied forward modeling techniques (FEM) to determine whether the underlying multivariate signal contained continuous tuning characteristics, and whether these differed for contingent and non-contingent. All BDM and FEM analyses were conducted using the Amsterdam Decoding and Modeling Toolbox (ADAM, Amsterdam, the Netherlands, Fahrenfort et al., 2018), which uses EEGLAB as input format and internally uses FieldTrip to perform time-frequency analysis.

Backward Decoding Model (BDM)

A backward decoding model was used to predict at which of the eight possible locations the cue was presented, based on the distribution of EEG activity (raw EEG and time-frequency power distributions - alpha). The underlying logic of this analysis is that if a trained classifier can predict with above-chance classification accuracy where the cue was presented, then it follows that location specific information is present in the distributed EEG patterns.

In order to conduct the BDM analyses on the data, a number of steps were taken to ensure the validity of the model. First, the trial order was randomized offline for every subject, to prevent order effects from affecting classifier performance in any way. Next, each subject's individual dataset was analyzed using a 10-fold cross-validation training-testing scheme. In this scheme, the data was segmented into 10 equally sized folds (each fold containing a near-equal number of trials, with equal distributions of the eight cue positions across the folds). A linear discriminant classifier was trained on 90% of the data (9 of the 10 folds), learning to discriminate between the different stimulus classes (i.e., the eight possible cue locations) separately for each of the two cue types. The validity of the trained classifier was tested on the left-out 10% of the data (the remaining fold); a procedure which was repeated ten times, such

that all data was tested once without ever using the same data for training and for testing. Separate decoding analyses were conducted using (1) the distributed amplitudes of the raw EEG signal over each electrode and time point and (2) the induced power of decomposed frequency information at each electrode and time point. Using 20 electrodes thus resulted in 20 features for eight stimulus classes (eight cue locations), classified in two conditions (contingent and non-contingent cues). Rather than using the average proportion of correctly classified stimulus categories as a performance measure (e.g. Fahrenfort et al., 2017), the BDM analyses used a slightly more sensitive performance measure by assessing the area under the curve (AUC; Hand and Till, 2001) of a Receiver-Operator Characteristic (ROC) that plots the cumulative probabilities that the classifier assigns to instances coming from the same class (i.e. the correct cue location) against the cumulative probabilities that the instance is classified as being from a different class (i.e. one of incorrect cue locations). As more than two classes (i.e. the cue location) were used, AUC was defined as the average AUC of all pairwise comparisons between classes. Using AUC as a performance measure is more sensitive than using decoding accuracy as it uses single trial confidence scores (i.e. the distances from the decision boundary) to compute performance, rather than averaging the performance on a set of binary classifier decisions. AUC typically runs from 0.5 (chance performance) to 1 (perfect performance).

Forward Encoding Models (FEMs)

Compared to BDMs, forward encoding models (FEMs; Brouwer and Heeger, 2009) take the opposite approach by establishing the continuous relationship between a stimulus parameter (cue position in this case) and multivariate neural patterns. This relationship is expressed in a single so-called Channel Tuning Function (CTF, loosely reminiscent of tuning properties of single neurons), which together with regression weights obtained during model creation allows one to reconstruct neural patterns for stimulus parameters that were never used to create the model (Fahrenfort et al., 2017; Brouwer and Heeger, 2009). Hence, the term 'forward model' reflects the fact that one can go from the stimulus parameter space to predict neural activity (and vice versa).

During FEM model fitting, a similar 10-fold procedure is used as during backward decoding analyses, but using a different procedure. First, a basis set is created for each of eight hypothetical channels reflecting cue position, and which describe the assumed (hypothetical) relationship between neural activity and the eight cue positions on the screen. The nomenclature "channels" here should not be confused with MEG or EEG sensors, EEG sensors are referred to as electrodes in the current manuscript. We used a Gaussian shaped basis set, which was created using a standard Gaussian function with an amplitude of 1 and a sigma of 1. Next, linear regression-based weight estimation for each of the hypothetical location channels was performed separately for each of the 20 features, specifying the one-to-one and invertible relationship between a particular cue position and the distributed multivariate neural response in the training set. Next, these weights were multiplied with trials in the testing set to produce the estimated channel responses for each trial in the testing set. This procedure was repeated for each of the 10 testing folds so that channel responses were derived once for each trial in all folds. Subsequently, the trial-based channel responses were averaged across trials in the testing set, separately for trials reflecting each of the eight different cue locations. The averaged channel responses in combination with the derived channel weights describe the validated and inversible relationship between attended cue location and the multivariate EEG response. In a final step, the eight estimated channel responses were aligned to a common center such that all eight channel responses were similarly centered. This step was conducted separately for each of the two cue conditions and was repeated for each time point, resulting in a CTF-over-time. The full procedure has been described at length in a number of other papers, both in mathematical terms (Brouwer and Heeger, 2009; Foster et al., 2016; Garcia et al., 2013; Samaha et al., 2016) as well as using more verbal and visual de-
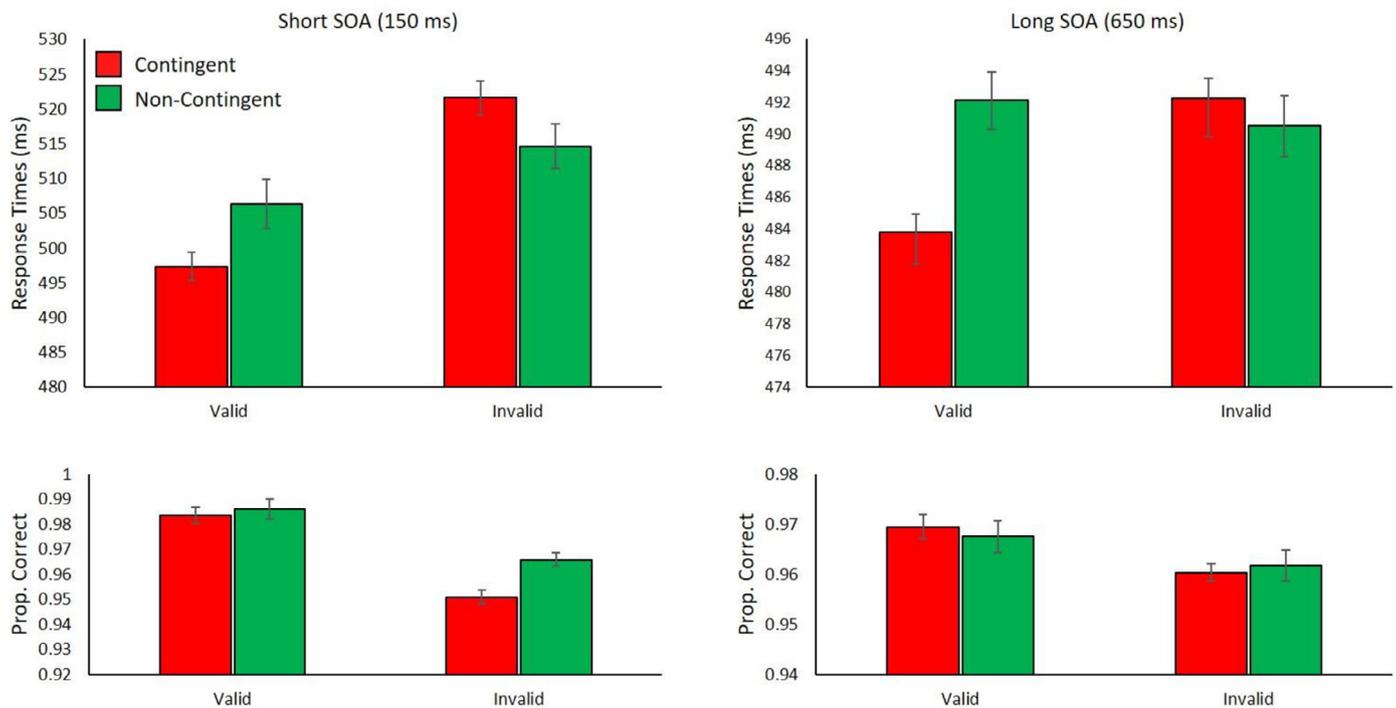
Fig. 2. Mean reaction times (top) and accuracy scores (bottom) for the different experimental conditions. Separate plots are shown for trials with short (left) and long (right) SOAs. Error bars reflect the 95% confidence interval (Cousineau, 2005; Morey, 2008).

scriptions (Fahrenfort et al., 2017; Foster, Sutterer, et al., 2017). As in the BDM analyses, separate FEM analyses were conducted using the distributed raw EEG signal and the induced power spectra as input.

Event-related potentials

To provide additional context to the interpretation of any effects observed in our phase-locked encoding and decoding analyses, we further established the 'traditional' cue evoked event-related potentials (ERPs) from 100 ms pre-cue until 1000 ms post-cue, separately for contingent and non-contingent cues. Of particular interest were peaks commonly associated with the early neural response to visual stimulation, such as the P1; an attention modulated positive deflection in originating in the contralateral hemisphere and occurring approximately 100 ms after the onset of a visual event (e.g. Luck et al., 1990). In addition, the aforementioned N2pc will be investigated as well. ERPs were derived from the averaged lateralized (contra- vs ipsilateral) responses using electrodes PO7 and PO8.

Results

Behavioral results

Reaction times

Only trials with correct responses were used in the reaction time analyses (5.23% discarded). Furthermore, for all analyses, trials with response times shorter than 200 ms as well as reaction times that were two standard deviations above the subject's conditional means were removed (4.11% discarded). To investigate the effect of cue contingency on attentional allocation to the target presented in the search array, we first calculated the mean reaction times per condition for trials with a short SOA (150 ms). The time course in this condition best reflects the classic studies on contingent capture and allows us to draw conclusions about cue-induced attentional effects on target selection. Fig. 2 (top panels) shows the mean reaction times and accuracy scores to targets preceded by valid and invalid cues, separately for contingent and non-contingent trials. A repeated-measures ANOVA on reaction times with

these factors showed a main effect of validity, indicating that participants were faster on trials in which the location of the cue matched the location of the target, compared to when cue and target were presented at different locations ($F(1,28) = 22.182$, $p < .001$, $\eta_p^2 = .442$). No main effect of contingency was observed ($F < 1$), but as expected, a clear interaction between contingency and validity was observed ($F(1,28) = 6.889$, $p = .014$, $\eta_p^2 = .197$), with post-hoc t-tests showing that the validity effect was larger on contingent trials (Δ 24 ms; $t(28) = 5.211$, $p < .001$) as compared to non-contingent trials (Δ 8 ms; $t(28) = 1.836$, $p = .077$).

A similar analysis was conducted for trials with a longer SOA (650 ms) in order to see if any of the cue-induced capture effects lingered such that it would influence the reaction times to targets presented with a larger temporal separation from the cue. No main effect of validity was observed ($F(1,28) = 2.826$, $p = .104$, $\eta_p^2 = .092$), suggesting that some of the attentional effects may have dissipated by the time the target was presented. Furthermore, a significant effect of contingency was observed ($F(1,28) = 4.292$, $p = .048$, $\eta_p^2 = .133$), with faster reaction times for contingent compared to non-contingent trials (see Fig. 2 for means). Finally, similar to the analysis on the short SOA data, an interaction between contingency and validity ($F(1,28) = 11.528$, $p = .002$, $\eta_p^2 = .292$) was found. Post-hoc testing showed that this interaction was driven by the presence of a validity effect on contingent trials (Δ 8 ms; $t(28) = 3.604$, $p = .001$) that was completely absent on non-contingent trials (Δ –2 ms; $t(28) = 0.607$, $p = .549$).

Accuracy

Overall accuracy was relatively high: 94.60% correct. An ANOVA on the mean accuracy scores with contingency and validity as factors for the short SOA trials (150 ms) showed a main effect of validity, indicating that participants were more accurate on trials with validly cued targets as compared to trials with invalidly cued targets ($F(1,28) = 33.795$, $p < .001$, $\eta_p^2 = .547$; See Fig. 2 – bottom panels for accuracy scores). A main effect of contingency was observed, indicating that participants responded less accurately on trials in which the target was preceded by a contingent compared to a non-contingent cue ($F(1,28) = 8.976$, $p = .006$, $\eta_p^2 = .243$). A significant interaction between contingency and validity
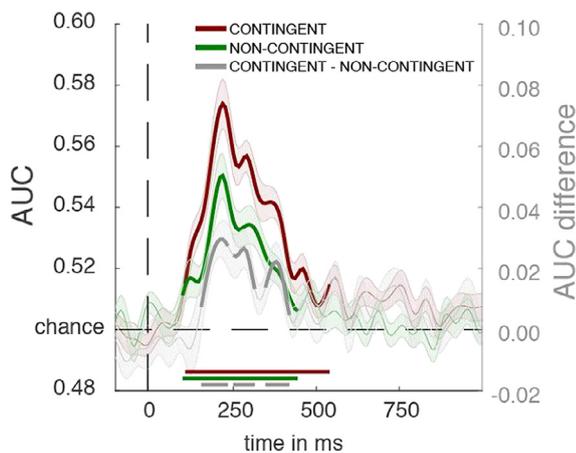
Fig. 3. Classification accuracy using BDM, expressed as Area Under the Curve (AUC) for contingent (red) and non-contingent (green) trials as well as their difference (grey), based on the raw EEG signal. Colored bars on the x-axis show the intervals where classification performance is above chance level (50.0%). Significant differences between contingent and non-contingent classification performance can be observed in multiple clusters ranging from 156 to 420 ms after cue onset ($T_{cue} = 0$).

was observed ($F(1,28) = 4.212$, $p < .001$, $\eta_p^2 = .547$), showing larger differences in accuracy between valid and invalid trials for contingent (3.27%; $t(28) = 5.126$, $p < .001$) as compared to non-contingent trials (2.0%; $t(28) = 4.639$, $p < .001$). A similar ANOVA on the trials with long SOAs (650 ms) showed only a significant main effect of validity, indicating that participants were overall more accurate on trials with validly cued targets as compared to invalidly cued targets ($F(1,28) = 6.748$, $p = .015$, $\eta_p^2 = .194$). No main effect of contingency ($F(1,28) = 1.613$, $p = .215$, $\eta_p^2 = .054$), nor an interaction between the two factors was observed ($F(1,28) = 1.907$, $p = .178$, $\eta_p^2 = .064$). Accuracy results need to be interpreted tentatively as the absence of hypothesized effects may be masked or distorted by a ceiling effect due to the overall high accuracy of most of the subjects.

EEG results

Raw EEG analysis (BDM)

To first establish whether we could find early effects of attentional capture (i.e., the effects in the N2pc domain) and to gauge the extent to which these effects are shaped by cue contingency, we applied a backward decoding analysis to determine cue position using the raw EEG signal (similar to Fahrenfort et al., 2017b). Fig. 3 shows classification accuracy (i.e. decoding accuracy as indexed by the ROC's area under the curve) over time, indicating the extent to which the cue location could be predicted based on the multivariate raw EEG patterns. Classification accuracy (AUC) was tested against chance level (50%), separately for trials containing contingent (red) and non-contingent (green) cues. T-tests against chance were conducted for every time sample in the epoched data, correcting for multiple comparisons using 1000-iteration cluster-based permutation tests (see Maris and Oostenveld, 2007). As can be observed from Fig. 3, both contingent (red) and non-contingent (green) cues yielded significant above-chance decoding performance (cluster-based $p < .05$, two-sided) emerging in the same time window as classical N2pc effects peaking between 200-250 ms after cue onset. To directly compare whether classification performance differed for contingent and non-contingent cues, classification performance for both cue types were tested against each other using paired samples t-tests. Again, these tests were conducted for each time point in the cue target interval, using cluster-based permutation testing to mitigate the multiple comparisons problem. Fig. 3 shows the difference between classification performance for contingent and non-contingent trials (grey line / right axis; i.e., con-

tingent – non-contingent) and clear significant differences for contingent compared to non-contingent cues can be observed in three consecutive temporal intervals (smallest cluster-based $p < .001$, one-sided), starting shortly after cue onset (156 ms after cue onset) and ending well before the target appeared (420 ms after cue onset). Note that the peak difference of the difference wave is consistent with the time of maximum classification accuracy for both contingent and non-contingent cues.

Time–frequency analysis (BDM)

We applied a backward decoding analysis to the time-frequency data, aimed at investigating to what extent the multivariate distribution of the EEG's power spectra could be used to predict at which location the contingent and non-contingent cues were presented. Past work has shown that this approach can track sustained orienting of covert attention, thereby providing an important complement to the analysis of the phase-locked EEG activity that appears to be most sensitive to attention effects occurring early after visual stimulation. Crucially, although separate multivariate analyses were conducted using the distribution of activity in the raw EEG on one hand and the distribution of power spectra amplitudes on the other hand, both measures were derived from the same data set and the same interval was tested for differential effects of the two cue types.

A first step in using distributed power spectra to decode the cue locations consisted of determining which neural oscillatory frequencies could be effectively used to decode this information. Therefore, a BDM analysis was conducted on all frequencies ranging from 2 to 30 Hz (in steps of 2 Hz; see Methods), separately for trials with contingent and with non-contingent cues. Fig. 4 shows the over time performance of the classifier averaged over cue location, based on the induced power spectra. Note that the induced signal does not contain any of the phase-locked evoked responses that are present in the raw EEG data (see Methods for details). As expected, the highest decoding accuracy was observed in the alpha-band range for both contingent (Fig. 4(A)) and non-contingent (Fig. 4(B)) cues (Foster et al., 2016). As such, we used this frequency band (8–12 Hz) to further examine whether we could decode the location of the different cue types based on time-frequency information.

Fig. 4(C) shows the above-chance classifier accuracy for contingent and non-contingent cues based on the distribution of alpha power over the scalp (red and green lines). Results showed that both contingent and non-contingent trials yielded above-chance classifier performance starting at approximately 250 ms post-cue and extending well past target onset ($T_{target} = 650$ ms). Crucially, the difference between contingent and non-contingent trials, as indicated by the grey line, was observed to be significant only in the later stages of the trial during an interval ranging from 596 ms to 860 ms post cue (cluster-based $p = .036$, one-sided).

Thus, these results show that the location of both the contingent as well as the non-contingent cues could effectively be decoded from the distributed pattern of alpha power over an extended period of time following cue onset, with contingent cues yielding significantly higher decoding accuracy later in the trial (shortly before target onset). When directly comparing the decoding accuracy based on alpha power for contingent and non-contingent cues, it appears that location tuning declined more quickly for non-contingent cues than for contingent cues. To further investigate whether a more specific model could bring out these differences between the two conditions we applied an FEM model to the raw EEG and the time-frequency data.

Raw EEG analysis (FEM)

The early above-chance classifier performance for contingent and non-contingent cue locations was taken as an incentive to investigate whether a forward encoding model (FEM) could be used to create location-selective channel tuning functions (CTFs) that describe the continuous relationship between multivariate patterns of EEG activity and cue location, separately for contingent and non-contingent cues. As raw
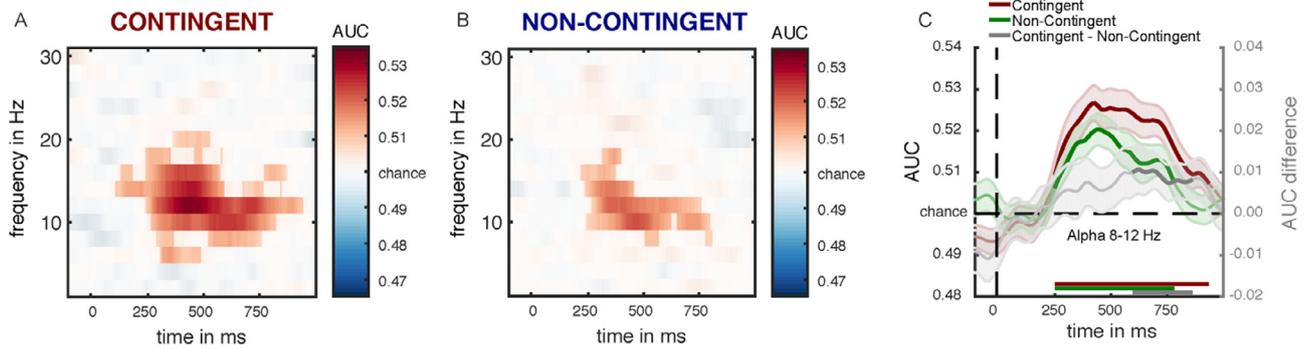
Figure 4. Classifier performance based on decomposed frequency power for frequencies ranging from 2 to 30 Hz (in steps of 2 Hz) for (**A**) contingent and (**B**) non-contingent (B) trials. Saturated values are cluster-corrected using cluster-based permutation testing (*p* < .05). (**C**) Classifier accuracy over time based on 8-12Hz alpha-band power independently for contingent and non-contingent data. Green and red bars at the *x*-axis indicate the regions of above-chance decoding accuracy. The grey bar indicates the difference in decoding accuracy between contingent and non-contingent cues (scaled on the grey axis on the right). The difference between contingent and non-contingent is significant in an interval ranging from 596 to 860 ms after cue onset.
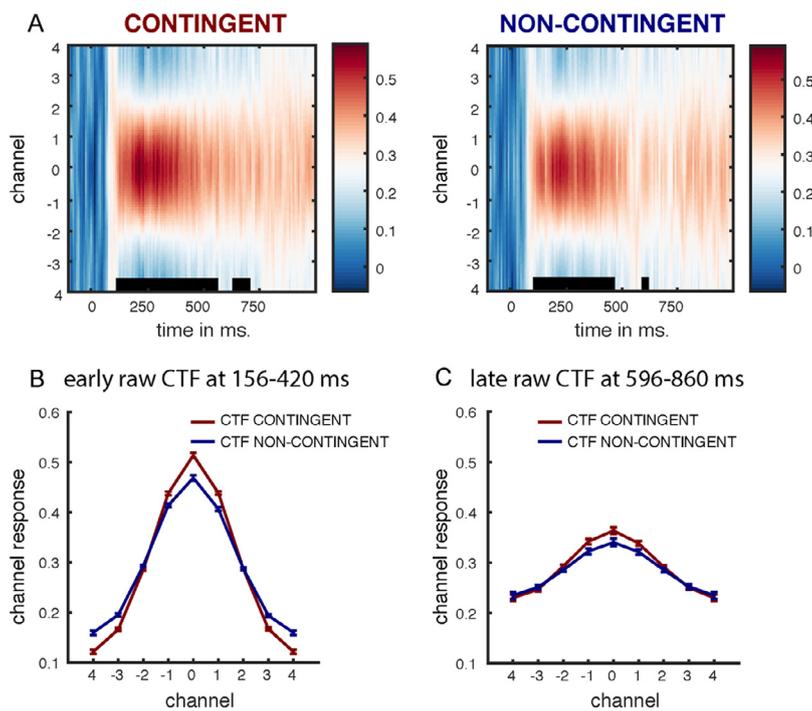

Fig. 5. (**A**) Development of channel tuning functions from cue onset ($T_{cue} = 0$) based on raw EEG data. Significance is indicated by black bars on the *x*-axes. (**B**). Contingent and non-contingent slope for the *early* time interval (156–420 ms after cue onset). (**C**) Contingent and Non-Contingent slope for the *late* time window (596–860 ms after cue onset).

EEG is used as input for the forward model, we expect any differences between contingent and non-contingent to arise as early effects in the channel tuning response over time, reflecting early and automatic effects of contingent capture.

A forward encoding model that describes the relationship between the multivariate EEG patterns and cue location (separately for cue type) was constructed (see Methods). Fig. 5(A) shows how the CTFs for contingent and non-contingent cues develop in a 1000 ms time window following cue onset. Significance testing of the CTFs was conducted by testing the slopes of the CTF function against 0 for each time point, again corrected for multiple comparisons using cluster-based permutation testing (*p* < .05). The slope of each CTF was estimated using linear regression after collapsing across channels that were equidistant from the channel tuned to the cued location (i.e., channels -4 and 4, channels -3 and 3, etc. as reported in Fig. 5). Significant periods in the developing CTFs are indicated by black bars at the bottom of the plots. As can be seen for both contingent and non-contingent cues, CTFs reach significance shortly after cue onset (approximately after 150 ms), dovetailing the observed time course of the BDM results using the raw EEG data.

To investigate whether the created forward encoding model describes a continuous relation between cue location and early and late effects of attentional capture, we compared the strength (i.e. the slopes) of contingent and non-contingent cue-induced tuning functions for the early and late intervals derived from the BDM analysis (i.e. early: 156–420 and late: 596–860). Fig. 5(B) and (C) shows the channel tuning functions for contingent and non-contingent cues for these intervals. We investigated the differences in the CTFs for contingent and non-contingent cues by directly comparing the slopes of each of the obtained functions to each other. In line with the BDM decoding results, the slopes of the evoked CTFs were statistically different for contingent and non-contingent cues in the early interval. A paired samples t-test showed that contingent cues resulted in steeper slopes as compared to non-contingent cues, showing that CTFs were more strongly tuned to the location of contingent compared non-contingent cues ($t(28) = 5.990$, $p < .001$). No such differences were observed in the late interval ($t(28) = 0.852$, $p = .401$), mirroring the results of the raw EEG BDM analyses. Thus, early effects of attentional capture were at modulated by the match between cue color and attentional set.
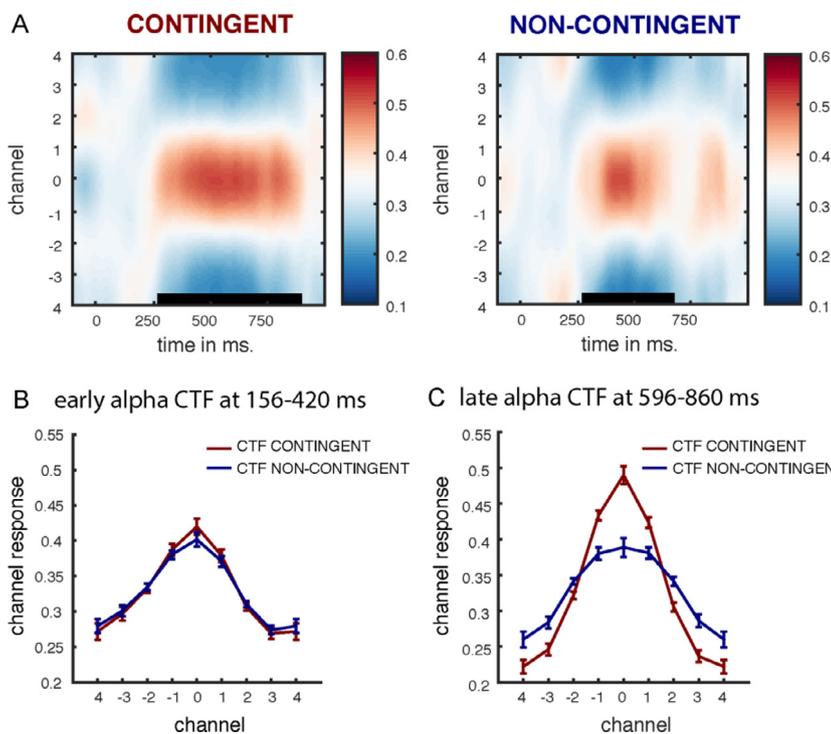
Fig. 6. (**A**) Development of channel tuning functions from cue onset based on alpha-band power. Significance is indicated by black bars on the *x*-axes. (**B**) Contingent and non-contingent slope for the *early* time interval (156–420 ms post-cue). (**C**) Contingent and Non-Contingent slope for the *late* time window (596–860 ms post-cue).

Time–frequency analysis (FEM)

We subsequently investigated whether a direct and continuous relationship could be established between cue location and the distributed pattern of alpha activity over the scalp. Similar to FEMs based on raw EEG data, and utilizing the same data set, channel tuning functions were created separately for contingent and non-contingent cues. As shown in Fig. 6(A), a strong relationship between cue location and induced alpha power was observed yielding robust channel tuning functions for both contingent and non-contingent cues.

Following the results obtained in the BDM analyses and the procedure conducted for the FEM analysis on the raw data, we distinguished between early (156–420 ms post-cue) and late (596–860 ms post cue) intervals, to expose temporal differences between the neural response to contingent and non-contingent cues, as encoded in the distributed alpha power. Contrary to the raw EEG encoding results, no difference in slope was observed for the early interval (Fig. 6(B); $t(28) = 0.459$, $p = .650$), suggesting that alpha power did not encode any differences in early, automatic attentional modulation of the cues. As expected, a significant slope difference between contingent and non-contingent cues was observed in the late interval ($t(28) = 2.970$, $p = .006$), with contingent cues yielding a steeper slope as compared to non-contingent cues. The results presented in Fig. 6(B) further suggest that there is no difference between the slopes evoked by non-contingent cues in the early compared to the late time interval. However, this lack of an effect is caused by the observation that alpha does not yield strong CTFs early on in the selected time window (> 156 ms), resulting in equally strong CTFs compared to the late time window (the time windows being defined by the BDM analyses and not by the observations presented in Fig. 6(A)).

Analyses of raw EEG and alpha power revealed distinct time courses for the differences between contingent and non-contingent cue conditions. When using the raw EEG signal in the FEM analyses, significant differences between the two cue types can be observed in the early interval (156–420 ms after cue onset), but these differences are no longer present during the late interval (596 – 860 after cue onset). The opposite time course was observed with alpha-band power, where reliable differences were observed in the late time interval but not during the early time window. To quantify this inverse pattern, a repeated measure
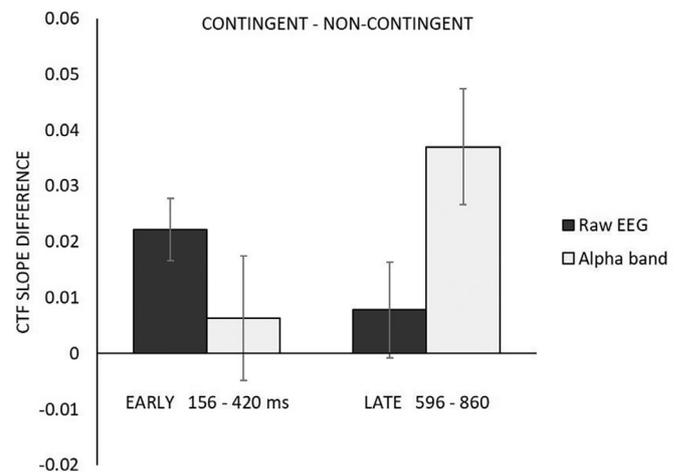

Fig. 7. The difference in CTF slopes for contingent and non-contingent cues. A clear interaction between signal type and interval can be observed. Error bars reflect the 95% confidence interval around the mean (Cousineau, 2005; Moray, 2008).

ANOVA was conducted on the individual slope values with contingency (contingent, non-contingent), time interval (early, late) and signal (raw EEG, alpha power). As main effects have already been established, the current results focus solely on the interactions between the different factors. First, the observed early/late reversal for raw EEG/alpha power is supported by a significant three-way interaction between contingency, time interval and signal type ($F(1,28) = 5.791$, $p = .023$, $\eta_p^2 = .171$). This interaction is illustrated in Fig. 7 in which the difference in CTF slope between contingent and non-contingent (contingent – non-contingent) is plotted as a function of time interval and signal type. Furthermore, a two-way interaction was observed between signal type and time interval, showing that raw EEG yielded steeper slopes in the early time interval as compared to the late time interval, whereas alpha-power resulted in the reversed pattern with steeper slopes in the late, compared
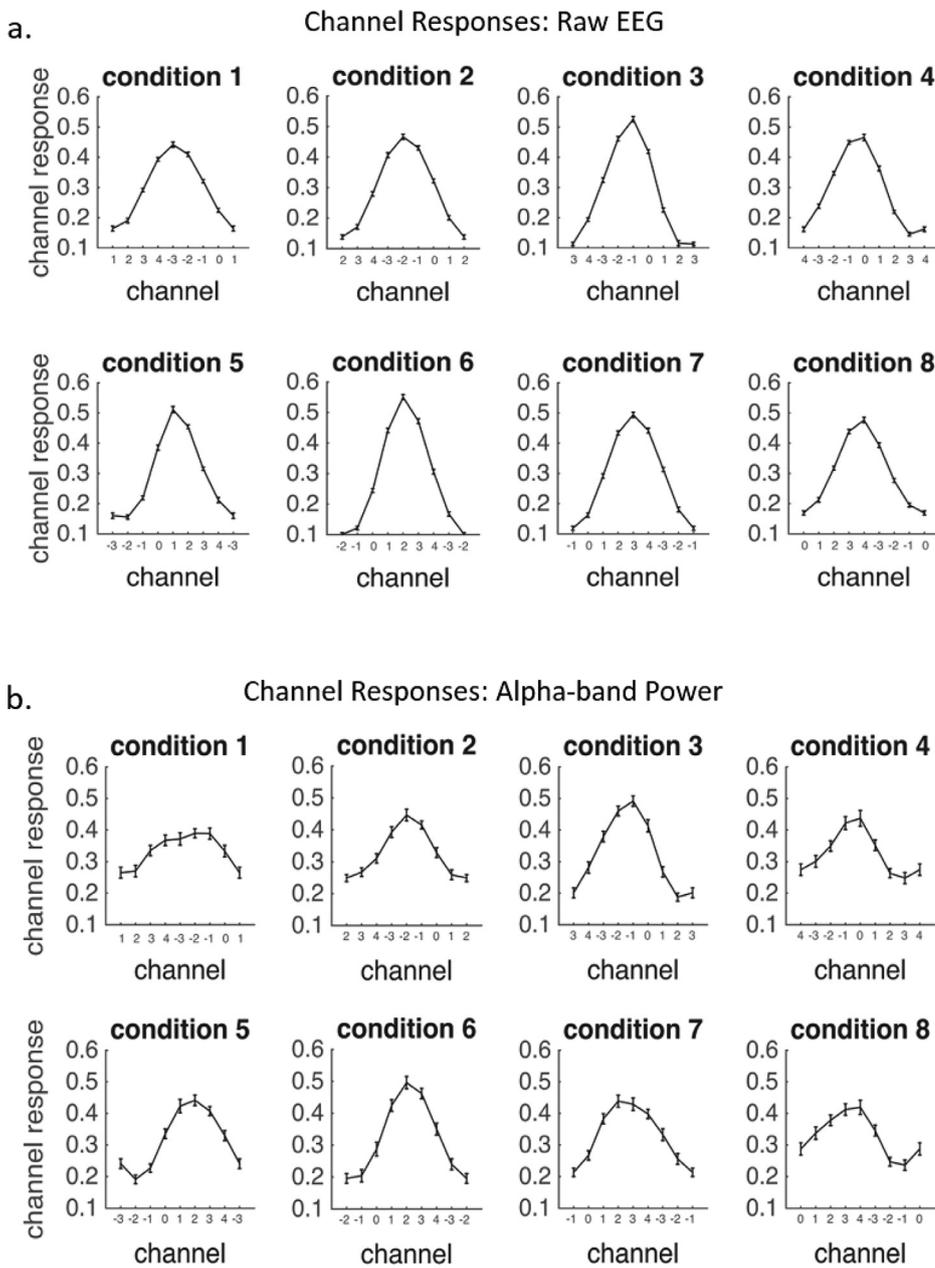
a.

Channel Responses: Raw EEG

b.

Channel Responses: Alpha-band Power

Fig. 8. Channel responses for individual conditions showing that the overall CTF is not driven by a subset of lateralized locations, but is based on a full spatial profile in which each location yields a distinct CTF. (A) location-based channel responses for early Raw EEG. (B) Location-based channel responses for alpha-band power.

to the early time interval ($F(1,28) = 31.629$, $p < .001$, $\eta_p^2 = .530$). These results imply that raw EEG and alpha power appear to track distinct cortical mechanisms related to the contingency between cue and target. No other interactions were observed.

To ensure that the observed encoding effects are based on a spatially graded profile for each condition (cue location) and to confirm that these effects were not driven by a subset of the cue locations, quadrants or hemifields, we plotted the averaged channel response for each condition separately for early Raw EEG (Fig. 8(A)) and late alpha power (Fig. 8(B)). As can be seen in Fig. 8, all locations showed a distinct location-specific CTF in both the raw EEG and the alpha power data, providing further evidence that the observed results (i.e. the difference between contingent and non-contingent cues) in this study indeed reflect location-specific effects of spatial attention.

Event-related potentials

To place the observed BDM and FEM effects in a broader and more traditional context, cue evoked event-related potentials were extracted

separately for contingent and non-contingent cues. In particular, we focused on early components of the visually evoked ERP that are known to be modulated by visual attention, such as the enhancement of the contralateral P1 component, as well as the N2pc component. Modulation of the N2pc is of particular interest as this component has been commonly associated with contingent attentional capture.

Similar to the multivariate analyses, the event-related responses to contingent and non-contingent cues were calculated for each participant and subsequently averaged in a 'grand-average' ERP response as plotted in Fig. 9. Again, *t*-tests against zero (baseline) were conducted for every time sample in the evoked potentials, correcting for multiple comparisons using 1000-iteration cluster-based permutation tests (alpha = .05). Direct comparison between the two cue conditions was likewise conducted using t-tests, testing differences between equal time samples in the two evoked potentials.

As can be seen in Fig. 9, results of the ERP analyses showed that both contingent and non-contingent cues elicited significant (above baseline) contralateral (compared to ipsilateral) enhancement of the P1 compo-
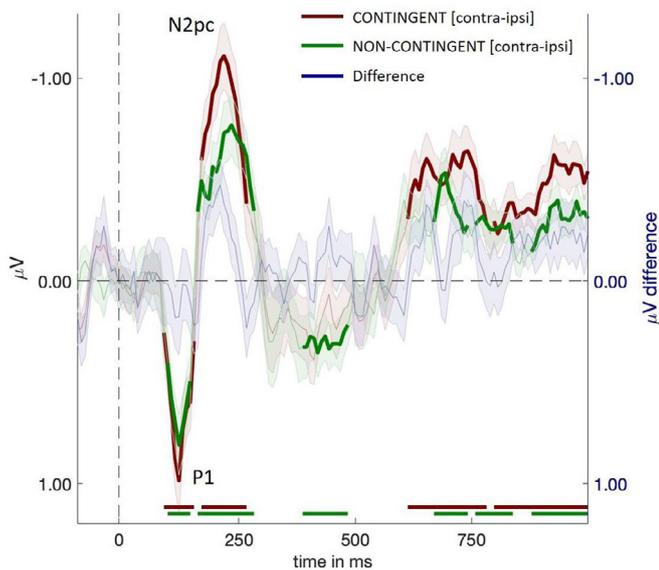
Fig. 9. Event related potentials for contingent and non-contingent cues ($T_{cue.} = 0$). Components that significantly differ from baseline (0) are indicated by the colored bars on the *x*-axes. Note that no difference between the two conditions was observed.

nents. The modulated P1 evoked by contingent cues showed a significant positive deflection ranging from 92 ms until 156 ms after cue onset, with a maximum amplitude at 124 ms after cue onset (cluster-based $p = .009$). Similarly, the non-contingent cue showed above baseline activity in the 100–148 ms time window following cue onset, with its peak amplitude measured at 124 ms following cue presentation (cluster-based $p < .009$). However, a direct comparison between the contralateral enhancement of the P1 evoked by contingent and non-contingent cues did not yield any significant differences, suggesting that both cue types elicited a similar neural response at this moment of processing.

In a similar fashion, both contingent and non-contingent cues evoked robust N2pc components, with the contingent cue showing a significant negative deflection ranging from 172 to 268 ms after cue onset, with the peak of the N2pc observed at 220 ms following cue onset (cluster-based $p < .001$). Non-contingent cues similarly evoked an N2pc observed in the 164–284 ms time window following cue onset, with the peak observed at 236 ms (cluster-based $p < .001$). However, in contrast to the decoding results no significant differences were observed between the contingent and non-contingent cue condition for these components. Do note that a one-tailed significant difference could be observed for the N2pc component, showing an increased amplitude for contingent, compared to non-contingent trials (time range: 180–228, cluster-based $p = .027$; not reported in Fig. 9). This analysis suggest that the decoding results are more sensitive indicators of the capture effects due to the multivariate nature of the ERP signal.

Discussion

The current study aimed to investigate the spatiotemporal properties of contingent capture. To this end, the full spatiotemporal profile of contingent capture was constructed via multivariate analysis of on-going EEG activity. This approach allowed us to examine attentional allocation in both early and late temporal intervals following the onset of contingent and non-contingent cues. Modulations of two well-known neurophysiological measures of attention were utilized to establish a direct relationship between attentional processes and neural activity: raw EEG and alpha-power.

Behaviorally, the data mirrored classic results observed in studies that provide support for contingent capture (Egeth and Yantis, 1997;

Folk et al., 1992; Folk and Remington, 1998, 2006). Reaction times to the target were influenced by the nature and location of the preceding cue, such that contingent cues exerted a strong influence on reaction times to the target, with reaction times depending on whether they were presented at the location of the target (fast RTs) or elsewhere in the display (slow RTs). This behavioral effect was strongly attenuated for non-contingent cues to the point where non-contingent cues did not produce a reliable RT difference between cues at the target location and cues elsewhere in the display. EEG analyses based on the raw EEG signal provided a clear difference between patterns of neural activity for contingent compared to non-contingent cues, in the early time interval, suggesting that more attentional resources were allocated to the contingent cue. Furthermore, during the late interval a similar difference between contingent and non-contingent cues was observed as measured using alpha power. Surprisingly, the non-contingent cues elicited above-chance decoding accuracy in this late time interval providing compelling evidence that this is *not* an effect that can be attributed to simple stimulus-driven feedforward processing, both given the late occurrence and the nature (alpha, which is indicative of feedback rather than feedforward; e.g. Doesburg et al., 2016) of the effect. The occurrence of such a late effect of non-contingent capture is novel and has to our knowledge not been previously reported in the literature. However, whether this effect reflects non-contingent capture itself, or is an unintended consequence of capture cannot be fully resolved from the current experiment.

Potential differences in the underlying neural mechanisms responsible for processing the contingent and non-contingent cues were assessed in two ways: First, following Fahrenfort et al. (2017) and Myers et al. (2015), the multivariate distribution of peak values in the raw EEG signal was used to show early and automatic effects of contingent capture. In addition, following Foster et al. (2017, 2016), distributed alpha power was used to test the allocation of spatial attention when faced with contingent and non-contingent cues. Backward decoding models were utilized to derive the location of the different cues based on the distributed neural EEG signal, whereas forward encoding models were used to establish a direct and continuous relationship between observed systematic EEG patterns and cue location, separately for each cue type.

By capitalizing on qualitatively different neurophysiological markers in the EEG signal (i.e. the raw EEG data and alpha power), the current study argues against the extreme version of both goal-driven and stimulus-driven models of attentional capture. The results of the current study distinguish between two neural signals known to track the deployment of covert attention. In line with previous work, the multivariate analyses based on the raw EEG (BDM and FEM) showed that the influence of attention emerged shortly after cue onset, but showed its strongest effect in the multivariate EEG patterns around 200–250 ms post cue. This peak time interval matches that of the well-established N2pc component (Eimer, 1996; Luck and Hillyard, 1994) and has repeatedly been linked to general attentional processes, such as identifying and localizing potential target stimuli embedded in an array of non-targets (Eimer, 1996; Hickey et al., 2006; Luck and Hillyard, 1994; Mazza et al., 2009) and more specifically to contingent capture (Grubert et al., 2017; Eimer, 1996; but see Hickey et al., 2006 for a bottom-up account). Nonetheless, differences in decoding between contingent and non-contingent cues can be observed as early as 156 ms after cue onset, preceding the classic N2pc time course which shows its earliest effects around 180 ms after stimulus onset. The most likely explanation for this effect is that the N2pc signal is modulated by an earlier bottom-up signal, evoked by the presentation of the singleton cue stimulus. Therefore, the observed above-chance decoding accuracy is hypothesized to be generated by the same evoked neural activity that is responsible for generation of the N2pc, but precedes it as it is modulated by an earlier bottom up signal. This finding has been substantiated by a recent study by Fahrenfort et al. (2017) in which a forward encoding model (based on raw EEG) was used to describe the continuous relationship between different target locations and systematic fluctuations

in neural patterns that arose in the N2pc time window. The current results dovetail those by Fahrenfort and colleagues, by showing a similar continuous relationship between potential cue location and systematic fluctuations in the distribution of the raw EEG peaks in the N2pc time window. However, contrary to Fahrenfort et al., the current results not only showed this relationship for contingent trials, but a similar albeit weaker observation was observed for non-contingent cues. This latter finding is most likely caused by properties of the experimental design in which the used cues are the only colored and salient stimuli in the display therefore strongly capturing attention in a bottom-up fashion. Furthermore, as these cue displays were asymmetrical (due to the presented color cue), it is likely that such displays evoke lateralized early visual responses (Clark et al., 1994), which could contribute to the above chance decoding accuracy for raw EEG based analyses.

The results of the FEM analysis focused on alpha power converged with those from the BDM analysis. Steeper CTF slopes were observed for contingent as compared to non-contingent cues in the late time window defined in the alpha-based BDM analysis. This observation contrasts with a recent study by Harris and colleagues (Harris et al., 2017) who showed that alpha-band oscillations were most strongly associated with attentional processes related to contingent cues, but not to non-contingent cues, whereas theta band activity (4–8 Hz) was associated with capture of both cue types, with stronger effects for contingent cues. However, Harris and colleagues investigated alpha and theta oscillatory activity as a function of early attentional capture, focusing on early effects of attention following cue presentation. In our analysis, relatively early (~250 ms after cue onset) decoding of cue position was observed in alpha activity, but differences in attention to contingent and non-contingent cues were not observed until a later time interval which coincided with the onset of the target stimulus.

The observed late effects in the difference between neural activity underlying processing of contingent and non-contingent cues may reflect slower disengagement from contingent relative to non-contingent cue locations. As argued by Theeuwes et al. (2000) disengagement from the cue may be fast when the cue and the target do not share the same defining properties, while disengagement is slow when cue and target have the same defining features (see also Belopolsky et al., 2010; Fukuda and Vogel, 2009; Grubert et al., 2017). Theeuwes et al. (2000) showed that it takes only about 100–150 ms to disengage attention from a cue that does not match the target feature one is searching for.

An alternative and speculative interpretation of the observed late effects in the alpha-based analyses follows recent literature that suggests a link between alpha power and endogenous processes (e.g. David et al., 2006; Hosseini et al., 2015). As such, the observed results tentatively suggest a role for slower, voluntary endogenous spatial attentional control that is possibly initiated by early effects of attentional capture. For example, the observed late effects in the difference between neural activity underlying the processing of contingent and non-contingent cues could potentially reflect the effort necessary to voluntarily disengage from an initially captured, but invalid cue location, with more attentional control being required from a location that contained a contingent cue, as compared to locations containing a non-contingent cue. Perhaps this endogenous signal can be more easily "turned off" when the presented cue has a low target-similarity as in the case of non-contingent cues. That is, observers can rapidly re-allocate spatial attentional resources once it is clear that the attended location does not contain the target. While this is a speculative interpretation of the late alpha based results, the current data suggests that disengaging attention from a target with high target-similarity appears to take more time and effort such that endogenous spatial attention to a contingent may still linger at the cued location when the target is presented (see also, Belopolsky et al., 2010; Grubert et al., 2017).

Nonetheless, while a role of endogenous attention seems appropriate around the moment of target onset, above-chance decoding accuracy based on alpha tuning was observed for both contingent and non-

contingent cues starting around 250 ms post cue. An interpretation in terms of voluntary attention seems problematic for this result, as it would not be beneficial to voluntarily attend to the largely uninformative cues (12.5% valid). As such, given the early onset of alpha-based modulations to both contingent and non-contingent cues, it appears that modulations of alpha activity may also reflect processes that are directly linked to early, involuntary bottom-up capture. The discrepancy between the current results and those observed by Harris and colleagues (Harris et al., 2017) is not immediately clear, but may be attributable to different types of analyses used to study spatial attention.

Interestingly, the observed event-related potentials do not completely fall in line with the results obtained using the multivariate raw EEG patterns. While a strong contralaterally enhanced P1 was observed following both contingent and non-contingent cues, no difference in the enhanced P1 magnitude was observed between these two conditions, as opposed to the presented multivariate raw EEG based analyses. However, this lack of a conditional effect is not out of line with earlier work that strongly suggests that the first ERP component modulated by contingent capture is the slightly later N2pc component (e.g. Eimer, 1996; Eimer and Kiss, 2008; Grubert et al., 2017). Similarly, the current study did not yield robust differences in N2pc amplitude between contingent and non-contingent cues, but a trend was observed in the expected direction, as indicated by a significant one-tailed t-test. Interestingly, whereas the N2pc effects are relatively weak, the decoding analysis based on the raw EEG data are fairly strong. Therefore, the current results do not only reflect on the nature of contingent capture, but also provide a strong case for multivariate EEG analysis, perhaps in combination with ERPs, as the more robust means of analyzing the time course of neuro-cognitive processes.

While our data show that contingent cues elicited stronger attentional capture, it may be premature to refer to this as an instance of "goal-driven" attention, because target color was held constant for each observer. Under these conditions, it has been established that selection biases will linger for the selected color even when the current goals of the observer have changed. This lingering effect is sometimes referred to as "selection history" (Awh et al., 2012), and it describes an interesting class of selection phenomena in which neither physical stimulus salience nor the current attentional goals of the observer can explain the selection bias (see also Theeuwes, 2018). A similar phenomenon can be observed in studies of value-driven capture showing that attention is involuntarily allocated to stimuli that are associated with obtaining a reward, even when the reward is no longer available and the value-signaling stimulus is not the target, ruling out an explanation in terms of top-down effects (Anderson, 2013; Anderson et al., 2011).

In sum, the current study shows that salient stimuli with features that either match or do not match a defining target feature evoke two consecutive but independent attentional signals. First, such stimuli elicit an 'early' effect in which attention appears to be captured by all salient stimuli, but with a stronger influence of attention for contingent compared to non-contingent stimuli. This early effect appears to function as input for a 'late' attentional mechanism that is potentially endogenous in nature and can be switched off when the attended location does not contain the sought-after target stimulus (or a stimulus closely matching that target). In line with the current results, Hopfinger and West (2006) have suggested that bottom-up and top-down attention can operate concurrently and interactively, by showing distinct and overlapping effects of attention on information processing. The current study elaborates on this finding by showing that attentional capture draws upon multiple attentional mechanisms to shape target selection and identification.

Credit author statement

Jaap Munneke: Responsible for all aspects of the presented research: Experimental design, data collection, data analysis and dissemination

Johannes Fahrenfort: Responsible for all aspects of the presented research, with a main focus on the computational data analysis and dis-

semination. This author contributed equally to the study compared to author 1

David Sutterer: Responsible for experimental design and data collection

Jan Theeuwes: Responsible for experimental design and dissemination

Ed Awh: Responsible for experimental design, data analysis and dissemination

Data and code availability statement

All data have been made publicly available via the Open Science Framework and can be accessed at https://osf.io/g2c5y. The used analysis code can be downloaded at https://github.com/fahrenfort/ADAM.

References

Anderson, B.A., 2013. A value-driven mechanism of attentional selection. J. Vis. 13 (3), 7. doi:10.1167/13.3.7.

Anderson, B.A., Laurent, P.A., Yantis, S., 2011. Value-driven attentional capture. Proc. Natl. Acad. Sci. 108 (25), 10367–10371. doi:10.1073/pnas.1104047108.

Awh, E., Belopolsky, A.V., Theeuwes, J., 2012. Top-down versus bottom-up attentional control: a failed theoretical dichotomy. Trends Cogn. Sci. 16 (8), 437–443. doi:10.1016/j.tics.2012.06.010.

Bacon, W.F., Egeth, H.E., 1994. Overriding stimulus-driven attentional capture. Percept. Psychophys. 55 (5), 485–496. doi:10.3758/BF03205306.

Belopolsky, A.V., Schreij, D., Theeuwes, J., 2010. What is top-down about contingent capture. Attent. Percept. Psychophys. 72 (2), 326–341. doi:10.3758/APP.72.2.326.

Brouwer, G.J., Heeger, D.J., 2009. Decoding and reconstructing color from responses in human visual cortex. J. Neurosci. 29 (44), 13992–14003. doi:10.1523/JNEUROSCI.3577-09.2009.

Clark, V.P., Fan, S., Hillyard, S.A., 1994. Identification of early visual evoked potential generators by retinotopic and topographic analyses. Hum. Brain Mapp. 2 (3), 170–187. doi:10.1002/hbm.460020306.

Cousineau, D., 2005. Confidence intervals in within-subject designs: a simpler solution to Loftus and Masson's method. Tuto. Quant. Methods Psychol. 1 (1), 42–45. doi:10.20982/tqmp.01.1.p042.

David, O., Kilner, J.M., Friston, K.J., 2006. Mechanisms of evoked and induced responses in MEG/EEG. NeuroImage 31 (4), 1580–1591. doi:10.1016/j.neuroimage.2006.02.034.

Delorme, A., Makeig, S., 2004. EEGLAB: an open source toolbox for analysis of single-trial EEG dynamics including independent component analysis. J. Neurosci. Methods 134 (1), 9–21. doi:10.1016/j.jneumeth.2003.10.009.

Doesburg, S.M., Bedo, N., Ward, L.M., 2016. Top-down alpha oscillatory network interactions during visuospatial attention orienting. NeuroImage 132, 512–519. doi:10.1016/j.neuroimage.2016.02.076.

Egeth, H.E., Yantis, S., 1997. Visual attention: control, representation, and time course. Annu. Rev. Psychol. 48 (1), 269–297. doi:10.1146/annurev.psych.48.1.269.

Eimer, M., 1996. The N2pc component as an indicator of attentional selectivity. Electroencephalogr. Clin. Neurophysiol. 99 (3), 225–234.

Eimer, M., Kiss, M., 2008. Involuntary attentional capture is determined by task set: evidence from event-related brain potentials. J. Cogn. Neurosci. 20 (8), 1423–1433. doi:10.1162/jocn.2008.20099.

Fahrenfort, J.J., Leeuwen, J.van, Olivers, C.N.L., Hogendoorn, H., 2017. Perceptual integration without conscious access. Proc. Natl. Acad. Sci., 201617268 doi:10.1073/pnas.1617268114.

Fahrenfort, J.J., van Driel, J., van Gaal, S., Olivers, C.N.L., 2018. From ERPs to MVPA using the Amsterdam decoding and modeling toolbox (ADAM). Front. Neurosci. 12. doi:10.3389/fnins.2018.00368.

Fahrenfort, J.J., Grubert, A., Olivers, C.N.L., Eimer, M., 2017. Multivariate EEG analyses support high-resolution tracking of feature-based attentional selection. Sci. Rep. 7 (1), 1886. doi:10.1038/s41598-017-01911-0.

Folk, C.L., Remington, R., 1998. Selectivity in distraction by irrelevant featural singletons: evidence for two forms of attentional capture. J. Exp. Psychol.: Hum. Percept. Perform. 24 (3), 847–858. doi:10.1037/0096-1523.24.3.847.

Folk, C.L., Remington, R., 2006. Top-down modulation of preattentive processing: testing the recovery account of contingent capture. Visu. Cogn. 14 (4–8), 445–465. doi:10.1080/13506280500193545.

Folk, C.L., Remington, R.W., Johnston, J.C., 1992. Involuntary covert orienting is contingent on attentional control settings. J. Exp. Psychol.: Hum. Percept. Perform. 18 (4), 1030–1044. doi:10.1037/0096-1523.18.4.1030.

Foster, J.J., Bsales, E.M., Jaffe, R.J., Awh, E., 2017. Alpha-band activity reveals spontaneous representations of spatial position in visual working memory. Curr. Biol.: CB 27 (20), 3216–3223. doi:10.1016/j.cub.2017.09.031.

Foster, J.J., Sutterer, D.W., Serences, J.T., Vogel, E.K., Awh, E., 2016. The topography of alpha-band activity tracks the content of spatial working memory. J. Neurophysiol. 115 (1), 168–177. doi:10.1152/jn.00860.2015.

Foster, J.J., Sutterer, D.W., Serences, J.T., Vogel, E.K., Awh, E., 2017. Alpha-band oscillations enable spatially and temporally resolved tracking of covert spatial attention. Psychol. Sci., 0956797617699167 doi:10.1177/0956797617699167.

Fukuda, K., Vogel, E.K., 2009. Human variation in overriding attentional capture. J. Neurosci. 29 (27), 8726–8733. doi:10.1523/JNEUROSCI.2145-09.2009.

Garcia, J.O., Srinivasan, R., Serences, J.T., 2013. Near-real-time feature-selective modulations in human cortex. Curr. Biol. 23 (6), 515–522. doi:10.1016/j.cub.2013.02.013.

Grubert, A., Fahrenfort, J., Olivers, C.N.L., Eimer, M., 2017. Rapid top-down control over template-guided attention shifts to multiple objects. NeuroImage 146, 843–858. doi:10.1016/j.neuroimage.2016.08.039.

Hand, D.J., Till, R.J., 2001. A simple generalisation of the area under the ROC curve for multiple class classification problems. Mach. Learn. 45 (2), 171–186. doi:10.1023/A:1010920819831.

Harris, A.M., Dux, P.E., Jones, C.N., Mattingley, J.B., 2017. Distinct roles of theta and alpha oscillations in the involuntary capture of goal-directed attention. NeuroImage 152, 171–183. doi:10.1016/j.neuroimage.2017.03.008.

Hickey, C., McDonald, J.J., Theeuwes, J., 2006. Electrophysiological evidence of the capture of visual attention. J. Cogn. Neurosci. 18 (4), 604–613. doi:10.1162/jocn.2006.18.4.604.

Hopfinger, J.B., West, V.M., 2006. Interactions between endogenous and exogenous attention on cortical visual processing. NeuroImage 31 (2), 774–789. doi:10.1016/j.neuroimage.2005.12.049.

Hosseini, P.T., Bell, S., Wang, S., Simpson, D., 2015. Induced activity in EEG in response to auditory stimulation. Biomed. Signal Process. Control 22, 31–43. doi:10.1016/j.bspc.2015.06.005.

Kim, M.-S., Cave, K.R., 1999. Top-down and bottom-up attentional control: on the nature of interference from a salient distractor. Percept. Psychophys. 61 (6), 1009–1023. doi:10.3758/BF03207609.

Leber, A.B., Egeth, H.E., 2006. It's under control: top-down search strategies can override attentional capture. Psychonom. Bull. Rev. 13 (1), 132–138.

Luck, S.J., Heinze, H.J., Mangun, G.R., Hillyard, S.A., 1990. Visual event-related potentials index focused attention within bilateral stimulus arrays. II. Functional dissociation of P1 and N1 components. Electroencephalogr. Clin. Neurophysiol. 75 (6), 528–542. doi:10.1016/0013-4694(90)90139-B.

Luck, S.J., Hillyard, S.A., 1994. Spatial filtering during visual search: evidence from human electrophysiology. J. Exp. Psychol. Hum. Percept. Perform. 20 (5), 1000–1014.

Maris, E., Oostenveld, R., 2007. Nonparametric statistical testing of EEG- and MEG-data. J. Neurosci. Methods 164 (1), 177–190. doi:10.1016/j.jneumeth.2007.03.024.

Mazza, V., Turatto, M., Caramazza, A., 2009. Attention selection, distractor suppression and N2pc. Cortex; J. Devot. Study Nervous Syst. Behav. 45 (7), 879–890. doi:10.1016/j.cortex.2008.10.009.

Morey, R.D., 2008. Confidence intervals from normalized data: a correction to Cousineau (2005). Tutor. Quant. Methods Psychol. 4 (2), 61–64.

Myers, N.E., Rohenkohl, G., Wyart, V., Woolrich, M.W., Nobre, A.C., Stokes, M.G., 2015. Testing sensory evidence against mnemonic templates. ELife 4, e09000. doi:10.7554/eLife.09000.

Oostenveld, R., Fries, P., Maris, E., Schoffelen, J.-M., 2010. FieldTrip: open source software for advanced analysis of MEG, EEG, and invasive electrophysiological data. Comput. Intell. Neurosci. 2011, e156869. doi:10.1155/2011/156869.

Samaha, J., Sprague, T.C., Postle, B.R., 2016. Decoding and reconstructing the focus of spatial attention from the topography of alpha-band oscillations. J. Cogn. Neurosci. 28 (8), 1090–1097. doi:10.1162/jocn_a_00955.

Schreij, D., Owens, C., Theeuwes, J., 2008. Abrupt onsets capture attention independent of top-down control settings. Percept. Psychophys. 70 (2), 208–218.

Schreij, D., Theeuwes, J., Olivers, C.N.L., 2010. Abrupt onsets capture attention independent of top-down control settings II: Additivity is no evidence for filtering. Attent. Percept. Psychophys. 72 (3), 672–682. doi:10.3758/APP.72.3.672.

Theeuwes, J., 1991. Cross-dimensional perceptual selectivity. Percept. Psychophys. 50 (2), 184–193.

Theeuwes, J., 1992. Perceptual selectivity for color and form. Percept. Psychophys. 51 (6), 599–606.

Theeuwes, J., 2004. Top-down search strategies cannot override attentional capture. Psychon. Bull. Rev. 11 (1), 65–70.

Theeuwes, J., 2018. Visual selection: usually fast and automatic; seldom slow and volitional. J. Cogn. 1 (1). doi:10.5334/joc.13.

Theeuwes, J., Atchley, P., Kramer, A.F., 2000. On the time course of top-down and bottom-up control of visual attention. Attent. Perform. 18, 104–124.

Wolfe, J.M., Butcher, S.J., Lee, C., Hyle, M., 2003. Changing your mind: on the contributions of top-down and bottom-up guidance in visual search for feature singletons. J. Exp. Psychol.: Hum. Percept. Perform. 29 (2), 483–502. doi:10.1037/0096-1523.29.2.483.